Behaviour of the von Willebrand Factor in Blood Flow

Kathrin MÜLLER[1*], Dmitry A. FEDOSOV[1], Gerhard GOMPPER[1]

1: Theoretical Soft Matter and Biophysics, Institute of Complex Systems and Institute for Advanced Simulation, Forschungszentrum Jülich, 52425 Jülich, Germany
* Corresponding author: Tel.: +49 (0)2461 613913; Fax: +49 (0)2461 613180; Email: k.mueller@fz-juelich.de

Abstract The von Willebrand factor (vWF), a large multimeric protein, is essential in hemostasis. Under normal conditions, vWF is present in blood as a globular polymer. However, in case of an injury, vWF is able to unwrap and bind to the vessel wall and to flowing platelets. Thus, platelets are significantly slowed down and can adhere to the wall and close the lesion. Nevertheless, it is still not clear how the unwrapping of the vWF is triggered. To better understand these complex processes, we employ a particle-based hydrodynamic simulation method to study the behaviour of vWF in blood flow. The vWF is modelled as a chain of beads (monomers) connected by springs. In addition, the monomers are subject to attractive interactions in order to represent characteristic properties of the vWF. The behaviour of vWF is investigated under different conditions including a freely-suspended polymer in shear flow and a polymer attached to a wall. We also examine the migration of vWF to a wall (margination) depending on shear rate and volume fraction of red blood cells (RBCs). Furthermore, the stretching of the vWF in flow direction depending on its radial position in a capillary is monitored. Our results show that attractive interactions between monomer beads increase margination efficiency and significantly affect the extension of vWF at different radial positions in blood vessels.

Keywords: Primary Hemostasis, Polymer, Margination Probability, Numerical Modelling, Dissipative Particle Dynamics

1 Introduction

As a response to a vascular injury, platelets are able to adhere at the damaged vessel wall to stop blood loss. The process of the initial platelet-plug formation is called primary hemostasis. Even though receptors on the surface of platelets can interact with several sub-endothelial ligands (e.g., collagen (Nuyttens et al., 2011)), platelet adhesion often still needs to be mediated by proteins such as the von Willebrand factor (vWF) (Ruggeri, 1997; Reininger, 2008; Schneppenheim and Budde, 2008), especially at high shear rates. For instance, for wall shear rates exceeding approximately $1500\,s^{-1}$, platelet velocities are too high for direct binding and their adhesion is practically mediated by vWF (Reininger, 2008).

vWF is the largest protein found in blood, with a contour length which can be larger than $100\,\mu m$ (Schneider et al., 2007; Dong, 2005). This multimeric protein is composed of identical subunits or dimers which have a length of approximately 70 nm and a thickness of about 10 nm. Assembled vWF can be released into the blood plasma, stored in the Weibel-Palade bodies, secreted basolaterally into the subendothelium, or stored in platelet α-granules. The stored vWF is often unusually long in comparison with plasmatic vWF. This ultralarge vWF (ULvWF) is typically released in response to signals which indicate vascular damages (Schneppenheim and Budde, 2008). ULvWF has been experimentally detected in blood plasma not only after an induced release from endothelial storage sites, but also in case of certain blood diseases (Reininger, 2008).

The adhesion of platelets to vWF is mediated by the glycoprotein Ibα (GPIbα) on

the surface of platelets. Platelet binding to vWF is able to withstand very high forces which would correspond to abnormally high shear rates and may occur in a stenosed (constricted) vessel (Reininger et al., 2006). However, GPIbα binding to immobilized vWF has high association as well as dissociation rates (Savage et al., 1996). Therefore, often platelets slide along the vWF chains in the direction of the flow (Maxwell et al., 2007). Their sliding velocity typically corresponds to about 2% of the velocity of freely flowing platelets. The slow velocity of sliding platelets facilitates the formation of bonds between platelets and sub-endothelial ligands (e.g., collagen) which lead to eventual platelet arrest (Savage et al., 1996; Reininger, 2008). Several experimental studies (Moake et al., 1986; Ruggeri, 1997, 2003; Barg et al., 2007) indicate that adhesion of platelets to vWF mainly depends on shear rate and the length of the vWF. These studies also suggest that an increased shear rate leads to a conformational change of vWF from a globular form to a stretched configuration, which is accompanied by increased platelet adhesion. Experiments with a single vWF in shear flow (Schneider et al., 2007) have shown that the average extension of vWF strongly depends on shear rate. vWF extension dramatically changes from a primarily globular configuration to a stretched one when a critical shear rate of about $5000\,\mathrm{s}^{-1}$ has been reached (Schneider et al., 2007). Furthermore, adhesion of a stretched vWF to exposed collagen at a site of injury is also enhanced. Recent numerical simulations and experiments on the formation of aggregates consisting of vWF and colloids in shear flow (Chen et al., 2013) have confirmed that vWF length, adhesive interactions, and shear rate are the most important factors which govern aggregate size.

A dysfunction of primary hemostasis can lead to extensive bleeding or undesired thrombotic events. One of the most common inherited bleeding disorders is the von Willebrand disease (vWD) with an incidence of up to 1% of the general population (Furlan, 1996). vWD can be caused by a reduced number of vWF chains or their complete absence. Other forms of the vWD are related to existing defects in vWF chains due to mutations leading to bleeding symptoms of different severity. A different type of blood disorder, thrombotic thrombocytopenic purpura, is caused by the dysfunction of vWF length regulation performed by the enzyme ADAMTS13, which normally cleaves long vWF chains and therefore, controls their length; this dysfunction leads to the occurrence of long vWF chains in blood plasma. As a result, spontaneous formation of vWF-platelet aggregates may occur and these small platelet clots (thrombi) can damage various tissues and organs due to blood-flow blockages (Schneppenheim et al., 2003).

Another important aspect of the primary hemostasis process is the availability of all necessary components near the site of injury, which is affected by their distribution within the vessel cross-section. Therefore, platelets and vWF have to migrate towards the wall through the process called margination. Particle margination in blood flow is mediated by red blood cells (RBCs), which migrate to the vessel center (Goldsmith et al., 1989) due to hydrodynamic interactions with the walls (called lift force) (Cantat and Misbah, 1999; Abkarian et al., 2002; Messlinger et al., 2009) leading to a RBC-free layer (RBCFL) near the walls. More precisely, the occurrence of margination is a consequence of the competition between lift forces on RBCs and suspended particles, and their interactions in flow (Kumar and Graham, 2012). The hydrodynamic interactions with the wall strongly depend on the deformability and size of suspended particles. For instance, the lift force on platelets is lower than that on RBCs since platelets are considerably stiffer and smaller than RBCs. As a result, vWF and platelets are expelled into the RBCFL, and thus occupy a position near the wall.

Numerical simulations of blood flow on the level of single cells (Fedosov et al., 2014) allow us to explore primary hemostasis and the margination process leading to a better understanding of the intricate interplay among blood

cells and vWF. Realistic simulations also contribute to the quantification of experimental data and elucidate physical and biological mechanisms involved. Using a mesoscopic hydrodynamics simulation approach, the behaviour of vWF in shear flow and blood flow is investigated. We study the extension of vWF and its margination properties. We find that adhesion of vWF to a wall leads to efficient vWF extension at shear rates substantially lower than the critical shear rate for the stretching of a freely flowing vWF. Furthermore, the globular form of vWF appears to be advantageous for its margination.

2 Models and methods

Simulation method. We employ the dissipative particle dynamics (DPD) method (Hoogerbrugge and Koelman, 1992; Español and Warren, 1995), a mesoscopic particle-based simulation approach, which properly captures hydrodynamics. The simulation system is represented by a collection of n point particles. The particles interact locally within a cutoff radius r_c through pairwise forces, which have conservative ($\mathbf{F}^C$), dissipative ($\mathbf{F}^D$), and random ($\mathbf{F}^R$) contributions. The time evolution of the velocity $\mathbf{v}_i$ and position $\mathbf{r}_i$ of particle i with the mass m_i is determined by the Newton's second law of motion $d\mathbf{r}_i = \mathbf{v}_i dt$ and $d\mathbf{v}_i = \frac{1}{m_i}\left(\mathbf{F}_i^C + \mathbf{F}_i^D + \mathbf{F}_i^R\right) dt$.

Red blood cell model. RBCs in 2D are modelled as a closed chain of N_s connected beads. The equilibrium distance between the beads is imposed by a spring potential. In addition, bending rigidity and area-conservation constraint are used for the RBC model. More details on the model can be found in Fedosov et al. (2012).

Simulation setup. The simulation setup consists of a slit geometry with a width of $W = 20\,\mu\text{m}$. In case of a single vWF polymer in shear flow, the length of a simulation box has been set to $L_C = 3.5W$, while for blood flow simulations $L_C = 6W$ has been employed. The channel was filled with fluid particles to model fluid flow and and with N_P suspended polymers. For blood flow simulations, N_{RBC} RBCs were suspended in addition to $N_P = 6$ polymers. The number of RBCs has been computed according to channel hematocrit H_t, which is defined as the area fraction of RBCs.

Boundary conditions. In flow direction, periodic boundary conditions were imposed, while in the other direction the suspension was confined by walls. The walls were modelled by frozen fluid particles having the same structure as the fluid, while the wall thickness was equal to r_c. Thus, the interactions of fluid particles with wall particles are the same as the interactions between fluid particles, and the interactions of suspended polymers and RBCs with the wall are identical to those with a suspending fluid. To prevent wall penetration, fluid particles as well as particles used for modelling RBCs and vWF are subject to reflection at the fluid-solid interface. We employed a bounce-back reflection rule, since it provides a better approximation for the no-slip boundary conditions in comparison to specular reflection of particles. To ensure that no-slip boundary conditions are strictly satisfied, a tangential adaptive shear force (Fedosov and Karniadakis, 2009) has been also added to act on the fluid particles in a near-wall layer of a thickness $h_c = r_c$.

System parameters. Shear flow has been obtained by moving the two walls in opposite direction with the same velocity magnitude. To characterize the flow strength for simple shear flow, we normalize the shear rate $\dot{\gamma} = \Delta v/W$ by the characteristic time scale $\tau = a^2\eta/k_BT$, where Δv is the velocity gradient between the walls, a is the monomer radius, η is the 2D dynamic viscosity, and k_BT is the energy scale.

Blood flow is driven by a constant force applied to each solvent particle, which is equivalent to a prescribed pressure gradient. To characterize the flow strength in this case, we define a non-dimensional shear rate as

$$\dot{\gamma}^* = \bar{\dot{\gamma}}\tau_{RBC} = \bar{\dot{\gamma}}\frac{\eta D_r^3}{\kappa_r}, \qquad (1)$$

where $\bar{\dot{\gamma}} = \bar{v}/W$ is the average shear rate (or pseudo shear rate) and $\bar{v}$ is the average flow velocity computed from the flow rate, while τ_{RBC} defines a characteristic RBC relaxation time. Here, $D_r = L_0/\pi$ is the effective RBC diameter with L_0 being the RBC contour length and κ_r is the RBC membrane bending rigidity. The RBCs are further characterized by the reduced area $A^* = 4A_0/(\pi D_r^2) = 0.46$, where A_0 is the enclosed RBC area. Typical values for real healthy RBCs are $D_r = 6.5\,\mu$m in 3D ($D_r = 6.1\,\mu$m in 2D), $\eta = 1.2 \times 10^{-3}$ Pa s, and $\kappa_r = 50 k_B T$ for the physiological temperature $T = 37\,^{\circ}$C.

Polymer (vWF) model. A polymer has been modelled as a bead-spring chain with a bead radius a as proposed by Alexander-Katz et al. (2006) and Schneider et al. (2007). The inter-bead interaction potential is given by

$$\frac{U_{\text{beads}}}{k_B T} = \kappa \sum_{i=1}^{N-1} (r_{i+1,i} - 2a)^2 + \quad (2)$$
$$+\epsilon \sum_{ij} \left(\left(\frac{2a}{r_{i,j}}\right)^{12} - 2\left(\frac{2a}{r_{i,j}}\right)^{6} \right),$$

where $r_{i,j} = r_i - r_j$ is the distance between two neighboring beads i and j. The first part of the potential corresponds to harmonic springs for inter-bead connections with an equilibrium spring length of $2a$. The second part is a Lennard-Jones (LJ) interaction with a strength ϵ, which imposes excluded-volume interactions between beads and may also add inter-bead attractive interactions. One type of a modelled polymer (repulsive polymer) employs only the repulsive part of the LJ potential with a cutoff distance of $r_{LJ} = 2a$. Other polymers (attractive polymer), which mimic the vWF, were modelled with the attractive part of the LJ potential, where the attraction strength ϵ has been varied. The polymer used in all simulations consisted of $N = 26$ beads corresponding to a length of $L = 15.6\,\mu$m.

3 Results

3.1 vWF extension in shear flow

To better understand the behaviour of vWF under shear, we studied the stretching of dif-

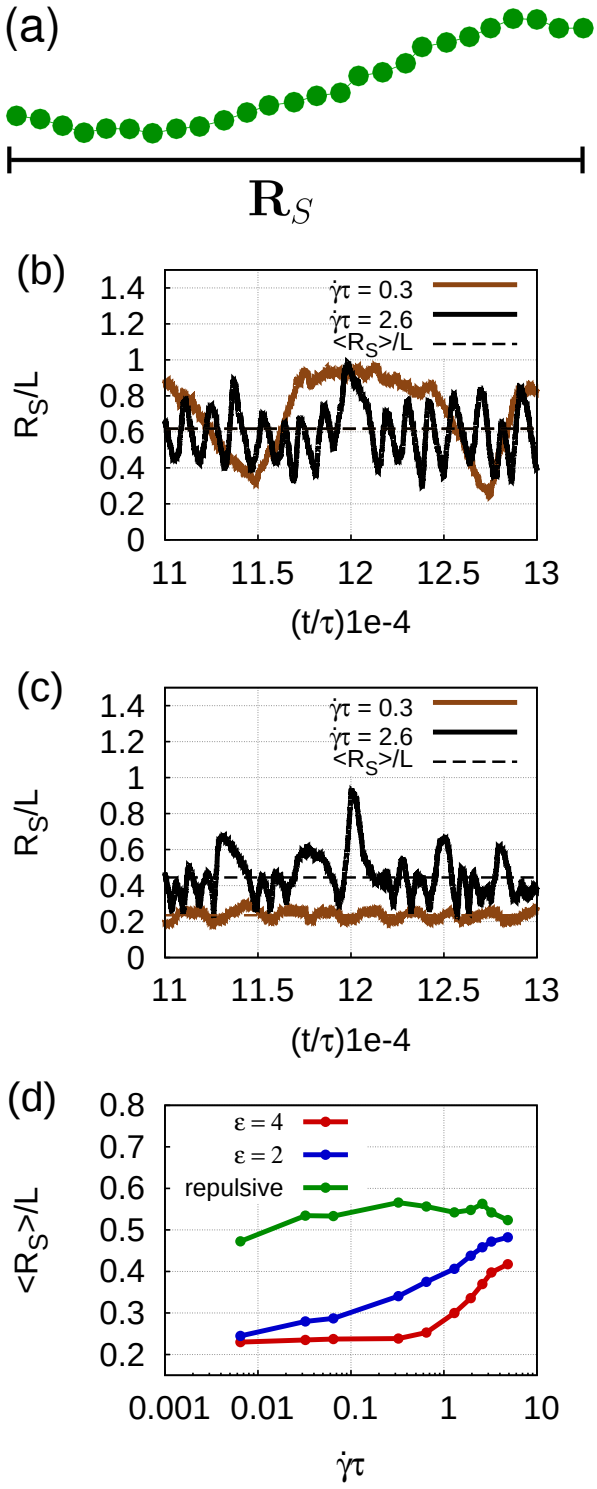

Figure 1: Polymer extension in shear flow. (a) A polymer snapshot with its extension R_S measured along the flow direction. (b) Time-dependent extension R_S for a repulsive polymer normalized by the contour length L. (c) Extension of an attractive polymer with $\epsilon = 4$ in shear flow. (d) Average extension $\langle R_S \rangle$ for the repulsive polymer model (green curve) and the attractive polymer model with $\epsilon = 2$ (blue curve) and $\epsilon = 4$ (red curve) depending on the shear rate $\bar{\dot{\gamma}}$ normalized by $\tau = a^2\eta/k_B T$.

ferent polymer models in shear flow, including a purely repulsive polymer, and a polymer with different LJ attraction strengths which mimic vWF inter-monomer interactions. Polymer stretching along the flow direction has been measured through the extension R_S depicted in Fig. 1(a). Under shear, polymers undergo a periodic stretch-and-tumble motion such that their extension due to the velocity gradient is followed by the tumbling and collapse, as studied extensively for repulsive polymers (Smith et al., 1999; Huang et al., 2011). Figures 1(b),(c) show the time dependence of R_S for the two polymer models and different shear rates. An increase in shear rate results in a higher rotational frequency which can be appreciated through the frequency of extension peaks in Fig. 1(b) for a repulsive polymer. An attractive polymer displays on average much lower extension than a repulsive polymer; furthermore, at low shear rates, the attractive polymer maintains its globular shape. Figure 1(d) presents the average extension $\langle R_S \rangle$ for these polymer models with respect to the normalized shear rate $\dot{\gamma}\tau$. For the investigated range of shear rates, a repulsive polymer shows a weak dependence of its extension on the shear rate, while an attractive polymer remains unstretched up to a critical shear rate. The critical shear rate as well as the width of globular-stretched transition strongly depends on ϵ. These results are in agreement with recent experiments and simulations of vWF in shear flow (Alexander-Katz et al., 2006; Schneider et al., 2007). A detailed quantitative comparison with experiments is difficult, since the simulation results are obtained for 2D systems. However, 2D systems provide interesting insights into the relevant mechanism.

Previous simulations have shown that polymer extension is more pronounced if it is located close to a wall (Alexander-Katz and Netz, 2007). Figure 2 presents our results which confirm this finding, but also illustrates the difference in extension between a freely-flowing polymer and a polymer attached to the wall. In comparison to a free polymer, the attachment to the wall results in an increased extension of both repulsive and attractive polymers for the same shear rate. For the attractive polymer adhered to the wall, the critical shear rate for stretching is about an order of magnitude lower than that for a free chain. In addition, platelet adhesion to vWF further facilitates its stretching.

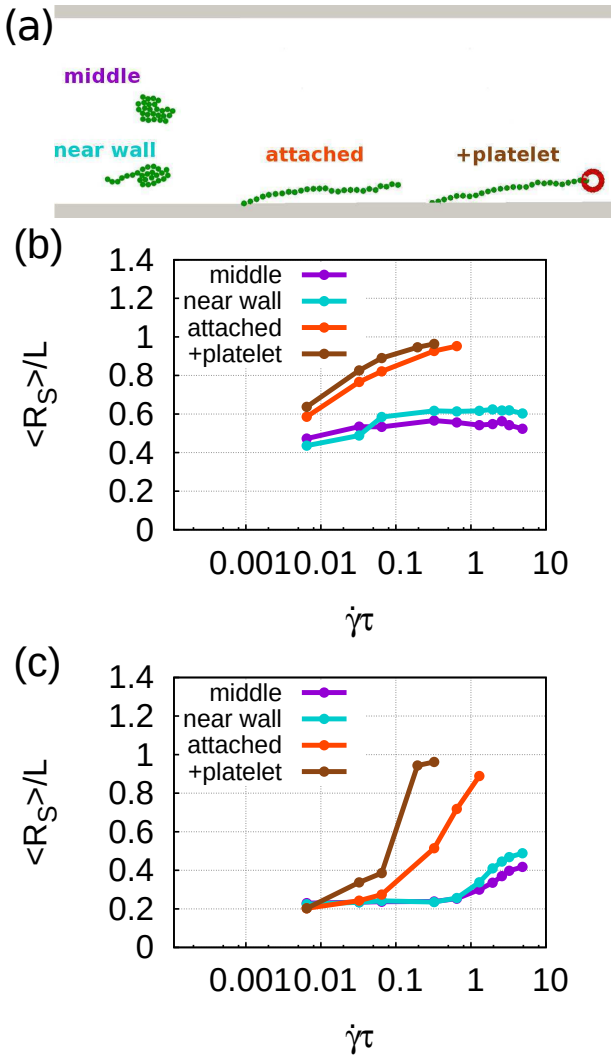

Figure 2: Polymer extension of adhered chains. (a) Combined snapshots of a polymer in simulations. Four different cases are investigated: polymer in the middle of a channel (purple), near a wall (cyan), anchored with its one end to the wall (orange), and anchored with its one end to the wall and a platelet attached to the other end (brown). Polymer average extension versus the normalized shear rate $\bar{\gamma}\tau$ for (b) the repulsive polymer and (c) the attractive polymer model with $\epsilon = 4$.

There also exist differences in dynamics of a free and attached polymer. The free polymer generally shows a cyclic transition between an

extended and a globular conformation during its rotation in shear flow, while the conformations of an attached polymer are quasi-extended and more stationary without significant stretching/recoiling dynamics.

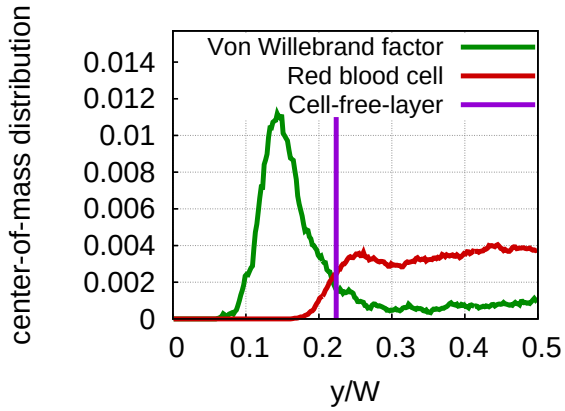

Figure 3: Center-of-mass probability distributions. The distributions of RBCs (red curve) and attractive polymers with $\epsilon = 4$ (green curve) across the channel for $H_t = 0.3$ and $\dot{\gamma}^* \approx 30$. The purple line indicates the width of the RBCFL.

3.2 vWF margination in blood flow

In order to elucidate the role of RBCs on vWF stretching and margination in blood flow, we investigate the behaviour of vWF under various blood flow conditions. Polymer positions in blood flow sampled over time supply us with distributions, which reflect the probability of a polymer to be at a certain distance from the wall. Figure 3 shows the center-of-mass distributions of vWF and RBCs for hematocrit $H_t = 0.3$ and the non-dimensional shear rate $\dot{\gamma}^* \approx 30$. The distributions were obtained for an attractive polymer model with $\epsilon = 4$. The RBCFL thickness which is computed from simulation snapshots through the analysis of the RBC core boundary (Fedosov et al., 2010) similar to experimental measurements (Kim et al., 2007). The distributions have been averaged over the halves of the channel due to symmetry. The results imply that the vWF migrates into the RBCFL and remains quasi-trapped there.

In order to quantify the margination, we define a margination probability as a fraction of

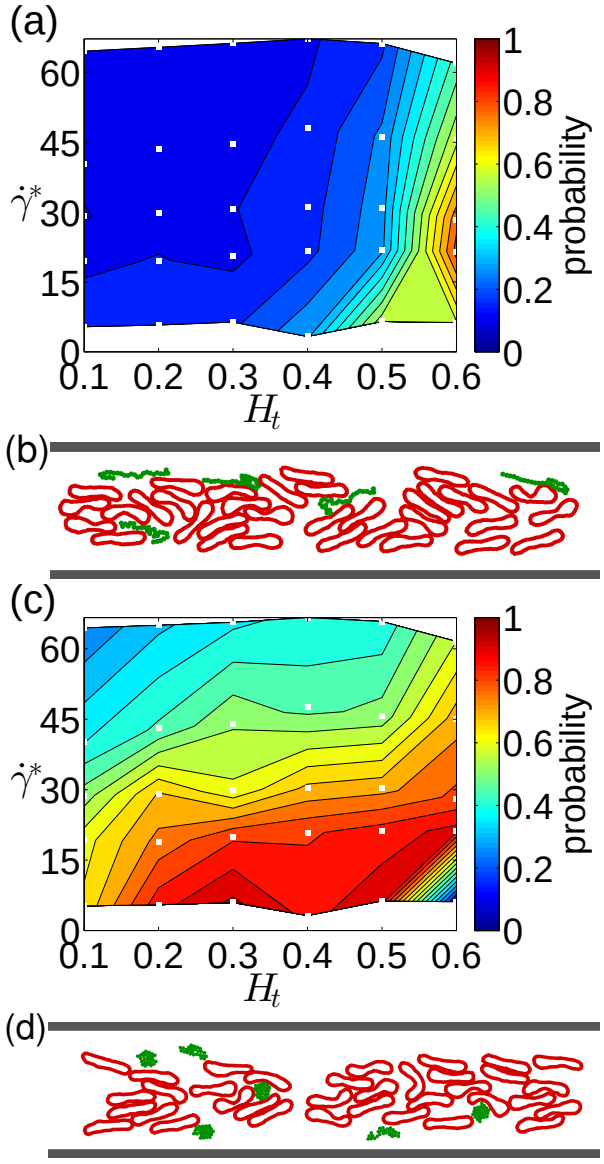

Figure 4: Margination probability diagrams. (a,c) Margination diagrams and (b,d) corresponding snapshots for the repulsive polymer model (a,b) and the attractive polymer model with $\epsilon = 4$ (c,d). The white squares indicate the values of hematocrit H_t and average shear rates $\dot{\gamma}^*$ for which simulations have been performed. The snapshots are for the system parameters $H_t = 0.3$ and $\dot{\gamma}^* \approx 30$.

suspended particles whose center of mass is located in a near-wall layer of thickness δ. Even though different choices of δ can be made, here we assume that δ is equal to the RBCFL thickness. Compilation of the margination probabilities for a wide range of hematocrits and shear rates leads to the construction of margination diagrams shown in Figs. 4 (a),(c). The margination diagrams indicate that the attractive poly-

mer marginates better than the repulsive one due to the different conformations of the polymers in flow. The repulsive polymer is fully flexible, and thus stretches more and experiences a stronger hydrodynamic repulsion from the wall than the attractive one. The snapshots in Figs. 4 (b),(d) illustrate that the polymer with attractive interactions is more compact in blood flow than the one with only repulsive interactions. However, both polymers marginate less efficiently than non-deformable particles with a comparable size (Müller et al., 2014).

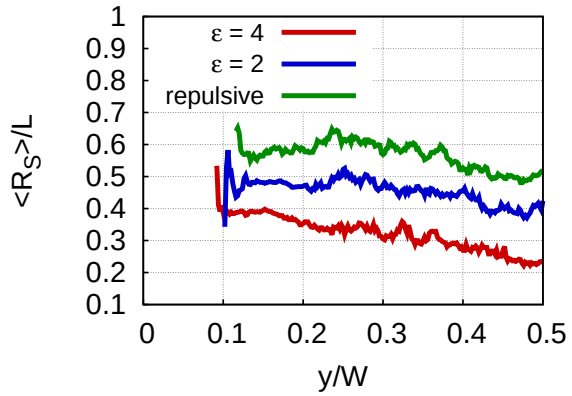

Figure 5: Polymer extension in blood flow. Average extension $\langle R_S \rangle$ normalized by the contour length L of the polymer at different center-of-mass positions y in the channel. The results are shown for the repulsive and attractive polymer models. Parameters here are $H_t = 0.4$ and $\dot{\gamma}^* \approx 48$.

The analysis of the average extension of the polymers with respect to their position across the channel reveals that the extension of the repulsive polymer is larger compared to the attractive one, see Fig. 5. However, near the wall the polymer extension increases in both cases. The difference between the lowest and the highest extension is larger for the attractive polymer. In addition, we find that the extension increases with increasing local shear rate in the channel, as observed for a single polymer in simple shear flow.

4 Summary

In order to better understand primary hemostasis, the behaviour of vWF and platelets, and their margination properties and interactions in blood flow have to be explored. For a single polymer in shear flow, a strong enough internal interaction leads to a model which is able to reproduce vWF behaviour found in experiments (Schneider et al., 2007). Adhesion of vWF to a wall results in its enhanced extension when compared to the freely flowing vWF at a same shear rate. Thus, the critical shear rate, at which considerable extension is observed, is also lower for an adhered vWF than for a freely flowing polymer. Consequently, an anchored vWF can expose binding sites for soluble vWF and platelets already at low shear rates, where no significant stretching of soluble vWF would occur.

Polymers with a higher internal attraction strength show better margination, since they are less deformable than repulsive polymers. Furthermore, the stretching of polymers with attractive internal interactions, which mimic vWF, depends on the local shear rate. Therefore, the extension increases close to the wall compared to the middle of the channel. Consequently, undesirable adhesion of platelets to vWF is unlikely in the bulk flow, whereas stretching of vWF close to the wall enables its binding to collagen, other anchored vWF, and platelets at a site of injury.

Acknowledgments

This work has been supported by the DFG Research Unit FOR 1543 “SHENC - Shear Flow Regulation in Hemostasis”. Dmitry A. Fedosov acknowledges funding by the Alexander von Humboldt Foundation. Kathrin Müller acknowledges support by the International Helmholtz Research School of Biophysics and Soft Matter (IHRS BioSoft). We also gratefully acknowledge a CPU time grant by the Jülich Supercomputing Center.

References

Abkarian, M., Lartigue, C., Viallat, A., 2002. Tank treading and unbinding of deformable vesicles in shear flow: determination of the lift force. Phys. Rev. Lett. 88, 068103.

Alexander-Katz, A., Netz, R. R., 2007. Surface-enhanced unfolding of collapsed polymers in shear flow. Europhys. Lett. 80, 18001.

Alexander-Katz, A., Schneider, M. F., Schneider, S. W., Wixforth, A., Netz, R. R., 2006. Shear-flow-induced unfolding of polymeric globules. Phys. Rev. Lett. 97, 138101.

Barg, A., Ossig, R., Goerge, T., Schneider, M. F., Schillers, H., Oberleithner, H., Schneider, S. W., 2007. Soluble plasma-derived von Willebrand factor assembles to a haemostatically active filamentous network. Thromb. Haemost. 97, 514–526.

Cantat, I., Misbah, C., 1999. Lift force and dynamical unbinding of adhering vesicles under shear flow. Phys. Rev. Lett. 83, 880–883.

Chen, H., Fallah, M. A., Huck, V., Angerer, J. I., Reininger, A. J., Schneider, S. W., Schneider, M. F., Alexander-Katz, A., 2013. Blood-clotting-inspired reversible polymer-colloid composite assembly in flow. Nat. Commun. 4, 1333.

Dong, J.-F., 2005. Cleavage of ultra-large von Willebrand factor by ADAMTS-13 under flow conditions. J. Thromb. Haemost. 3, 1710–1716.

Español, P., Warren, P., 1995. Statistical mechanics of dissipative particle dynamics. Europhys. Lett. 30, 191–196.

Fedosov, D. A., Caswell, B., Popel, A. S., Karniadakis, G. E., 2010. Blood flow and cell-free layer in microvessels. Microcirculation 17, 615–628.

Fedosov, D. A., Fornleitner, J., Gompper, G., 2012. Margination of white blood cells in microcapillary flow. Phys. Rev. Lett. 108, 028104.

Fedosov, D. A., Karniadakis, G. E., 2009. Triple-decker: Interfacing atomistic-mesoscopic-continuum flow regimes. J. Comp. Phys. 228, 1157–1171.

Fedosov, D. A., Noguchi, H., Gompper, G., 2014. Multiscale modeling of blood flow: from single cells to blood rheology. Biomech. Model. Mechanobiol. 13, 239–258.

Furlan, M., 1996. Von Willebrand factor: molecular size and functional activity. Ann. Hematol. 72, 341–348.

Goldsmith, H. L., Cokelet, G. R., Gaehtgens, P., 1989. Robin Fahraeus: evolution of his concepts in cardiovascular physiology. Am. J. Physiol. 257, H1005–H1015.

Hoogerbrugge, P. J., Koelman, J. M. V. A., 1992. Simulating microscopic hydrodynamic phenomena with dissipative particle dynamics. Europhys. Lett. 19, 155–160.

Huang, C.-C., Sutmann, G., Gompper, G., Winkler, R. G., 2011. Tumbling of polymers in semidilute solution under shear flow. Europhys. Lett. 93, 54004.

Kim, S., Kong, R. L., Popel, A. S., Intaglietta, M., Johnson, P. C., 2007. Temporal and spatial variations of cell-free layer width in arterioles. Am. J. Physiol. 293, H1526–H1535.

Kumar, A., Graham, M. D., 2012. Mechanism of margination in confined flows of blood and other multicomponent suspensions. Phys. Rev. Lett. 109, 108102.

Maxwell, M. J., Westein, E., Nesbitt, W. S., Giuliano, S., Dopheide, S. M., Jackson, S. P., 2007. Identification of a 2-stage platelet aggregation process mediating shear-dependent thrombus formation. Blood 109, 566–576.

Messlinger, S., Schmidt, B., Noguchi, H., Gompper, G., 2009. Dynamical regimes and hydrodynamic lift of viscous vesicles under shear. Phys. Rev. E 80, 011901.

Moake, J. L., Turner, N. A., Stathopoulos, N. A., Nolasco, L. H., Hellums, J. D., 1986. Involvement of large plasma von Willebrand factor (vWF) multimers and unusually large vWF forms derived from endothelial cells in shear stress-induced platelet aggregation. J. Clin. Invest. 78, 1456–1461.

Müller, K., Fedosov, D. A., Gompper, G., 2014. Margination of micro- and nano-particles in blood flow and its effect on drug delivery. Sci. Rep. 4, 4871.

Nuyttens, B. P., Thijs, T., Deckmyn, H., Broos, K., 2011. Platelet adhesion to collagen. Thromb. Res. 127, S26–S29.

Reininger, A. J., 2008. Function of von Willebrand factor in haemostasis and thrombosis. Haemophilia 14, 11–26.

Reininger, A. J., Heijnen, H. F. G., Schumann, H., Specht, H. M., Schramm, W., Ruggeri, Z. M., 2006. Mechanism of platelet adhesion to von Willebrand factor and microparticle formation under high shear stress. Blood 107, 3537–3545.

Ruggeri, Z. M., 1997. von Willebrand factor. J. Clin. Invest. 99, 559–564.

Ruggeri, Z. M., 2003. Von Willebrand factor, platelets and endothelial cell interactions. J. Thromb. Haemost. 1, 1335–1342.

Savage, B., Saldivar, E., Ruggeri, Z. M., 1996. Initiation of platelet adhesion by arrest onto fibrinogen or translocation on von Willebrand factor. Cell 84, 289–297.

Schneider, S. W., Nuschele, S., Wixforth, A., Gorzelanny, C., Alexander-Katz, A., Netz, R. R., Schneider, M. F., 2007. Shear-induced unfolding triggers adhesion of von Willebrand factor fibers. Proc. Natl. Acad. Sci. USA 104, 7899–7903.

Schneppenheim, R., Budde, U., 2008. von Willebrand disease and von Willebrand factor. UNI-MED Verlag AG, Bremen.

Schneppenheim, R., Budde, U., Oyen, F., Angerhaus, D., Aumann, V., Drewke, E., Hassenpflug, W., Häberle, J., Kentouche, K., Kohne, E., Kurnik, K., Mueller-Wiefel, D., Obser, T., Santer, R., Sykora, K.-W., 2003. von Willebrand factor cleaving protease and ADAMTS13 mutations in childhood TTP. Blood 101, 1845–1850.

Smith, D. E., Babcock, H. P., Chu, S., 1999. Single-polymer dynamics in steady shear flow. Science 283, 1724–1727.